*Quantum Electronics* **43** (12) 1132–1138 (2013) 

***TERAHERTZ RADIATION***

PACS numbers: 73.20.Mf; 52.35.Mw; 42.65.Re
DOI: 10.1070/QE2013v043n12ABEH015262

# Excitation of surface waves by a short laser pulse in a conductor

S.A. Uryupin, A.A. Frolov

***Abstract.*** **We have studied the possibility of exciting surface waves in a conductor, which is irradiated by a focused femtosecond laser pulse incident along the normal to the surface. The time-dependent ponderomotive force is shown to lead to the excitation of surface waves in the terahertz frequency range. It is also shown that the total energy and the pulse amplitude of the surface waves increases with increasing effective electron collision frequency.**

***Keywords:*** *surface wave, femtosecond laser pulse, terahertz frequency range, frequency of collisions.*

## 1. Introduction

Interest in the study of surface waves is caused not only by their unusual physical properties, but also by the possibility of using these waves in solving such important applications as diagnosis of the surface [1], generation of electron beams [2], and generation of terahertz radiation [3]. Linear theory of surface waves in conductors is extensively studied in the literature (see, e.g., books [1, 4] and references therein). Linear theory describes in great detail the laws of dispersion of the waves and the methods for their excitation. Nonlinear excitation methods have been studied to a much lesser extent. However, in experiments on the interaction of femtosecond laser pulses with conductors, when surface waves are excited along with the generation of harmonics [5] and terahertz radiation [6], there is a need to go beyond linear theory. The need to develop nonlinear theory of excitation of surface waves is, in particular, indicated in experiments [7, 8]. Nonlinear mechanisms of excitation of surface waves have been previously discussed, such as stimulated Compton scattering [9], instantaneous spatial modulation of the refractive index in the region of action of ultrashort laser pulses [10, 11], and parametric decay of the pump wave into two surface waves [12]. The author of [13] has developed the theory of nonlinear excitation of surface waves during the passage of the laser pulse through the plasma–vacuum interface.

In this paper, in contrast to [9]–[13], we consider another way of surface wave excitation in a conductor, which is realised under the ponderomotive action of focused pulsed laser radiation. The ponderomotive force generated by the laser pulse leads to the directed motion of electrons. In the skin layer of the conductor there appears a vortex current changing during the pulse action. This slowly varying current is the source of a low-frequency electromagnetic field, which is emitted from metal into the surrounding space. In Section 2 we present the necessary information about the shape and form of the incident pulse and the form of the ponderomotive potential in the conductor. The low-frequency field arising in the conductor due to the inhomogeneity and nonstationarity of the ponderomotive potential is studied in Section 3. The low-frequency field corresponding to a surface wave in vacuum is described in Section 4. In the same Section we have found the components of the Fourier transforms of the low-frequency field in vacuum and conductor. The energy distribution over the frequencies, the total energy and the magnetic field structure of the surface wave in the wave zone are described in Section 5 for the Gaussian pulse action on the conductor. It is shown that the energy distribution over the frequencies is bell-shaped, with a maximum near the frequency $\sim 1/\tau_*$, where $\tau_* = \tau\sqrt{1 + R^2/L^2}$, the time $\tau$ determines the Gaussian pulse duration $t_p = 2\tau\sqrt{\ln 2}$, $R$ is the size of the focal spot, $L = c\tau$ is the pulse length, and $c$ is the speed of light. The position of this maximum is almost independent of the collision frequency of electrons in the low-frequency field $\nu_s$. If $\nu_s\tau_* \ll 1$, the value of the maximum does not depend on $\nu_s$, and within the frequent collisions of electrons, when $\nu_s\tau_* \gg 1$, it increases proportionally to $\sqrt{\nu_s\tau_*}$. Consequently, the total energy of the surface wave also increases proportionally to $\sqrt{\nu_s\tau_*}$. We have found that the surface wave propagates in the form of an electromagnetic field pulse with a duration of the order of $\tau_*$.

## 2. High-frequency field and ponderomotive potential

Consider the irradiation of the conductor occupying the half-space $z > 0$ by the laser pulse propagating along the $z$ axis. We assume that the carrier frequency $\omega_0$ of the pulse is much larger than $1/\tau$ and radiation is weakly focused into the region whose characteristic size $R$ is much greater than $c/\omega_0$. Without significant loss of generality, we assume that the pulse has a Gaussian intensity distribution in the $xy$ plane. Under these assumptions, the electric field of the incident pulse has the form

$$\boldsymbol{E}_{\mathrm{L}}^{\mathrm{inc}}(\boldsymbol{r},t) = \frac{1}{2}\boldsymbol{E}_{\mathrm{L}}\left(t-\frac{z}{c}\right)\exp\left[-\mathrm{i}\omega_0\left(t-\frac{z}{c}\right)-\frac{\rho^2}{2R^2}\right]+\mathrm{c.c.} \quad (1)$$

**S.A. Uryupin** P.N. Lebedev Physics Institute, Russian Academy of Sciences, Leninsky prosp. 53, 119991 Moscow, Russia; National Research Nuclear University 'MEPhI', Kashirskoe sh. 31, 115409 Moscow, Russia; e-mail: uryupin@sci.lebedev.ru;
**A.A. Frolov** Joint Institute for High Temperatures, Russian Academy of Sciences, ul. Izhorskaya 13, Bld. 2, 125412 Moscow, Russia

Received 18 June 2013; revision received 5 September 2013
*Kvantovaya Elektronika* **43** (12) 1132–1138 (2013)
Translated by I.A. Ulitkin

where $\boldsymbol{E}_{\rm L}(t)$ is the electric field strength varying weakly during the time $\sim\tau$ on the $z$ axis; and $\rho=\sqrt{x^2+y^2}$; $\boldsymbol{r}=(\boldsymbol{\rho},z)$. We confine ourselves to consideration of the action of the field (1) under conditions when the carrier frequency $\omega_0$ of radiation and the electron collision frequency in the high-frequency field $\nu_{\rm h}$ satisfy the inequality

$$|\omega_0+{\rm i}\nu_{\rm h}|\gg|\kappa_{\rm L}(\omega_0)|v, \tag{2}$$

where $v$ is the characteristic velocity of the electrons and the wavenumber $\kappa_{\rm L}(\omega_0)$ determines the scale of variation of the field along the $z$ axis in the conductor $\delta\sim 1/|\kappa_{\rm L}(\omega_0)|$:

$$\kappa_{\rm L}(\omega_0)=\frac{\omega_0}{c}\sqrt{\frac{\omega_{\rm p}^2}{\omega_0(\omega_0+{\rm i}\nu_{\rm h})}-\varepsilon_0(\omega_0)}\,. \tag{3}$$

In formula (3), $\omega_{\rm p}$ is the plasma frequency, and $\varepsilon_0(\omega_0)=\varepsilon'_0(\omega_0)+{\rm i}\varepsilon''_0(\omega_0)$ is the contribution to the dielectric constant of the conductor of the bound electrons and lattice. Under these conditions, the field (1) produces in the conductor a nonuniform field

$$\boldsymbol{E}_{\rm L}(\boldsymbol{r},t)=\boldsymbol{E}_{\rm L}(t)\frac{\omega_0}{\omega_0+{\rm i}c\kappa_{\rm L}(\omega_0)}\exp\left[-{\rm i}\omega_0 t-\kappa_{\rm L}(\omega_0)z-\frac{\rho^2}{2R^2}\right]$$

$$+\,{\rm c.\,c.},\ z>0. \tag{4}$$

This field has a ponderomotive effect on the electrons. In the case when the carrier frequency $\omega_0$ significantly exceeds the frequency of collisions between the electrons $\nu_{\rm h}$, corresponding to the field (4), the ponderomotive potential has the form

$$\Phi(\boldsymbol{r},t)=\frac{e^2\boldsymbol{E}_{\rm L}^2(t)}{m|\omega_0+{\rm i}c\kappa_{\rm L}(\omega_0)|^2}\exp\left[-2\,{\rm Re}\,\kappa_{\rm L}(\omega_0)z-\frac{\rho^2}{R^2}\right], \tag{5}$$

where $e$ is the charge, and $m$ is the effective mass of the electron.

## 3. Low-frequency field in the conductor

The ponderomotive action of the pulse with a slowly time-varying amplitude of the field leads to the appearance of a low-frequency current and low-frequency field in the conductor. To determine the density of the low-frequency current, we will use the equation

$$\frac{\partial}{\partial t}\boldsymbol{j}(\boldsymbol{r},t)+\nu_{\rm s}\boldsymbol{j}(\boldsymbol{r},t)=\frac{\omega_{\rm p}^2}{4\pi}\left[\boldsymbol{E}(\boldsymbol{r},t)-\frac{1}{e}\nabla\Phi(\boldsymbol{r},t)\right], \tag{6}$$

where $\boldsymbol{E}(\boldsymbol{r},t)$ is low-frequency electric field in the conductor and $\nu_{\rm s}$ is the electron collision frequency in the low-frequency field, which differs from the frequency $\nu_{\rm h}$ due to the dependence of the frequency of electron–electron collisions on the field frequency [14]. To describe the low-frequency electromagnetic field, equation (6) must be supplemented by Maxwell's equations for the electric field $\boldsymbol{E}(\boldsymbol{r},t)$ and magnetic field $\boldsymbol{B}(\boldsymbol{r},t)$:

$${\rm rot}\boldsymbol{E}(\boldsymbol{r},t)=-\frac{1}{c}\frac{\partial}{\partial t}\boldsymbol{B}(\boldsymbol{r},t), \tag{7}$$

$${\rm rot}\boldsymbol{B}(\boldsymbol{r},t)=\frac{1}{c}\frac{\partial}{\partial t}\boldsymbol{D}(\boldsymbol{r},t)+\frac{4\pi}{c}\boldsymbol{j}(\boldsymbol{r},t), \tag{8}$$

where $\boldsymbol{D}(\boldsymbol{r},t)$ is the electric induction. When constructing the solution to equations (6)–(8), we use the Fourier transform with respect to time $t$ and coordinate $\boldsymbol{\rho}=(x,y)$:

$$\boldsymbol{F}(\boldsymbol{k}_\perp,z,\omega)=\int{\rm d}t{\rm d}\boldsymbol{\rho}\exp({\rm i}\omega t-{\rm i}\boldsymbol{k}_\perp\boldsymbol{\rho})\boldsymbol{F}(\boldsymbol{r},t),$$

$$\boldsymbol{F}(\boldsymbol{r},t)=\int\frac{{\rm d}\omega{\rm d}\boldsymbol{k}_\perp}{(2\pi)^3}\exp(-{\rm i}\omega t+{\rm i}\boldsymbol{k}_\perp\boldsymbol{\rho})\boldsymbol{F}(\boldsymbol{k}_\perp,z,\omega), \tag{9}$$

where $\boldsymbol{k}_\perp=(k_x,k_y)$ is the wave vector in the $xy$ plane, and $\boldsymbol{F}(\boldsymbol{r},t)$ is one of the functions $\boldsymbol{j}(\boldsymbol{r},t)$, $\boldsymbol{E}(\boldsymbol{r},t)$, $\boldsymbol{B}(\boldsymbol{r},t)$ or $\boldsymbol{D}(\boldsymbol{r},t)$. In virtue of the axial symmetry of the ponderomotive potential (5) the current density, the fields and the induction vector have the form

$$\boldsymbol{j}(\boldsymbol{r},t)=(j_\rho(\boldsymbol{r},t),0,j_z(\boldsymbol{r},t)),\ \boldsymbol{E}(\boldsymbol{r},t)=(E_\rho(\boldsymbol{r},t),0,E_z(\boldsymbol{r},t)),$$

$$\boldsymbol{B}(\boldsymbol{r},t)=(0,B_\varphi(\boldsymbol{r},t),0),\ \boldsymbol{D}(\boldsymbol{r},t)=(D_\rho(\boldsymbol{r},t),0,D_z(\boldsymbol{r},t)).$$

After the Fourier transform we obtain from equations (7) and (8) a system of equations for the Fourier transforms of the components of the electric and magnetic fields:

$$\frac{\rm d}{{\rm d}z}E_\rho(\boldsymbol{k}_\perp,z,\omega)-{\rm i}k_\perp E_z(\boldsymbol{k}_\perp,z,\omega)=\frac{{\rm i}\omega}{c}B_\varphi(\boldsymbol{k}_\perp,z,\omega),$$

$$-\frac{\rm d}{{\rm d}z}B_\varphi(\boldsymbol{k}_\perp,z,\omega)=-\frac{{\rm i}\omega}{c}\varepsilon_0(\omega)E_\rho(\boldsymbol{k}_\perp,z,\omega)+\frac{4\pi}{c}j_\rho(\boldsymbol{k}_\perp,z,\omega), \tag{10}$$

$${\rm i}k_\perp B_\varphi(\boldsymbol{k}_\perp,z,\omega)=-\frac{{\rm i}\omega}{c}\varepsilon_0(\omega)E_z(\boldsymbol{k}_\perp,z,\omega)+\frac{4\pi}{c}j_z(\boldsymbol{k}_\perp,z,\omega),\ z>0.$$

When transforming equation (8) we used the relationship of the Fourier transform of the induction vector and the electric field $\boldsymbol{D}(\boldsymbol{r},\omega)=\varepsilon_0(\omega)\boldsymbol{E}(\boldsymbol{r},\omega)$. Equations (6) and (10) are valid in the region $z>0$. Taking into account the explicit form of the ponderomotive potential (5), we extend these equations and the unknown functions in the region $z<0$:

$$B_\varphi(\boldsymbol{k}_\perp,-z,\omega)=-B_\varphi(\boldsymbol{k}_\perp,z,\omega),\ E_\rho(\boldsymbol{k}_\perp,-z,\omega)=E_\rho(\boldsymbol{k}_\perp,z,\omega),$$

$$E_z(\boldsymbol{k}_\perp,-z,\omega)=-E_z(\boldsymbol{k}_\perp,z,\omega),\ \Phi(\boldsymbol{k}_\perp,-z,\omega)=\Phi(\boldsymbol{k}_\perp,z,\omega), \tag{11}$$

$$j_z(\boldsymbol{k}_\perp,-z,\omega)=-j_z(\boldsymbol{k}_\perp,z,\omega),\ j_\rho(\boldsymbol{k}_\perp,-z,\omega)=j_\rho(\boldsymbol{k}_\perp,z,\omega).$$

Taking into account relations (11), from equation (6) after the Fourier transform with respect to time and coordinates we find the Fourier transform of the current density

$$j(\boldsymbol{k},\omega)=\frac{\rm i}{4\pi}\frac{\omega_{\rm p}^2}{(\omega+{\rm i}\nu_{\rm s})}\left[\boldsymbol{E}(\boldsymbol{k},\omega)-{\rm i}\frac{\boldsymbol{k}}{e}\Phi(\boldsymbol{k},\omega)\right]. \tag{12}$$

Below, using expressions (11), (12) and the Fourier transform in the coordinate $z$ [see (9)], from equations (10) we obtain the relations

$$k_z E_\rho(\boldsymbol{k},\omega)-k_\perp E_z(\boldsymbol{k},\omega)=\frac{\omega}{c}B_\varphi(\boldsymbol{k},\omega),$$

$$-{\rm i}k_z B_\varphi(\boldsymbol{k},\omega)+\Delta B_\varphi(\boldsymbol{k}_\perp,\omega)$$

$$=-\frac{{\rm i}\omega}{c}\varepsilon(\omega)E_\rho(\boldsymbol{k},\omega)+\frac{1}{c}\frac{\omega_p^2}{(\omega+{\rm i}\nu_{\rm s})}\frac{k_\perp}{e}\Phi(\boldsymbol{k},\omega), \tag{13}$$

$${\rm i}k_\perp B_\varphi(\boldsymbol{k},\omega)=-\frac{{\rm i}\omega}{c}\varepsilon(\omega)E_z(\boldsymbol{k},\omega)+\frac{1}{c}\frac{\omega_{\rm p}^2}{(\omega+{\rm i}\nu_{\rm s})}\frac{k_z}{e}\Phi(\boldsymbol{k},\omega),$$

where

$$\Delta B_\varphi(\boldsymbol{k}_\perp,\omega) = B_\varphi(\boldsymbol{k}_\perp, z=+0,\omega) - B_\varphi(\boldsymbol{k}_\perp, z=-0,\omega)$$
$$= 2B_\varphi(\boldsymbol{k}_\perp, z=+0,\omega)$$

is the jump of the function $B_\varphi(\boldsymbol{k}_\perp,z,\omega)$ on the plane $z = 0$ because of the odd continuation to the region $z < 0$;

$$\varepsilon(\omega) = \varepsilon_0(\omega) - \frac{\omega_p^2}{\omega(\omega + i\nu_s)} \tag{14}$$

is the dielectric constant of the conductor provided that $|\omega + i\nu_s| \gg kv$. The solution of the system of equations (13) for the components of the Fourier transforms of the electromagnetic field has the form

$$B_\varphi(\boldsymbol{k},\omega) = \frac{2ik_z c^2}{\omega^2\varepsilon(\omega) - k^2c^2} B_\varphi(\boldsymbol{k}_\perp, z=+0,\omega), \tag{15}$$

$$E_\rho(\boldsymbol{k},\omega) = \frac{2i\omega c}{k^2} B_\varphi(\boldsymbol{k}_\perp, z=+0,\omega)$$
$$\times\left[\frac{k_z^2}{\omega^2\varepsilon(\omega) - k^2c^2} + \frac{k_\perp^2}{\omega^2\varepsilon(\omega)}\right] - \frac{ik_\perp\omega_p^2}{\omega(\omega+i\nu_s)}\frac{\Phi(\omega,\boldsymbol{k})}{e\varepsilon(\omega)}, \tag{16}$$

$$E_z(\boldsymbol{k},\omega) = -B_\varphi(\boldsymbol{k}_\perp, z=+0,\omega)$$
$$\times\frac{2i}{\omega\varepsilon(\omega)}\frac{k_z k_\perp c^3}{\omega^2\varepsilon(\omega) - k^2c^2} - \frac{ik_z\omega_p^2}{\omega(\omega+i\nu_s)}\frac{\Phi(\omega,\boldsymbol{k})}{e\varepsilon(\omega)}. \tag{17}$$

Using the inverse Fourier transform in the coordinate $z$ [see (9)], from (15)–(17) we find an expression for the functions $B_\varphi(\boldsymbol{k}_\perp,z,\omega)$, $E_\rho(\boldsymbol{k}_\perp,z,\omega)$ and $E_z(\boldsymbol{k}_\perp,z,\omega)$ in the conductor:

$$B_\varphi(\boldsymbol{k}_\perp,z,\omega) = B_\varphi(\boldsymbol{k}_\perp, z=+0,\omega)\exp(-\kappa z), \tag{18}$$

$$E_\rho(\boldsymbol{k}_\perp,z,\omega) = \frac{ic\kappa}{\omega\varepsilon(\omega)} B_\varphi(\boldsymbol{k}_\perp, z=+0,\omega)\exp(-\kappa z)$$
$$-\frac{ik_\perp\omega_p^2}{\omega(\omega+i\nu_s)}\frac{\Phi(\boldsymbol{k}_\perp,z,\omega)}{e\varepsilon(\omega)}, \tag{19}$$

$$E_z(\boldsymbol{k}_\perp,z,\omega) = -\frac{ck_\perp}{\omega\varepsilon(\omega)} B_\varphi(\boldsymbol{k}_\perp, z=+0,\omega)\exp(-\kappa z)$$
$$-\frac{\omega_p^2}{\omega(\omega+i\nu_s)}\frac{\partial}{\partial z}\frac{\Phi(\boldsymbol{k}_\perp,z,\omega)}{e\varepsilon(\omega)}, \tag{20}$$

where

$$\kappa = \sqrt{k_\perp^2 - \omega^2\varepsilon(\omega)/c^2} = \kappa_1 - i\kappa_2;\ \varepsilon(\omega) = \varepsilon'(\omega) + i\varepsilon''(\omega);$$

$$\kappa_s = \frac{1}{c\sqrt{2}}\left\{\sqrt{\left[k_\perp^2c^2 - \omega^2\varepsilon'(\omega)\right]^2 + \left[\omega^2\varepsilon''(\omega)\right]^2}\right.$$
$$\left. -(-1)^s\left[k_\perp^2c^2 - \omega^2\varepsilon'(\omega)\right]\right\}^{1/2},\ s = 1, 2. \tag{21}$$

The quantity $1/\kappa_1$ determines the size of the localisation region of the low-frequency field in the conductor near its surface.

## 4. Low-frequency field in vacuum. Surface wave

The low-frequency electromagnetic field in vacuum, when $z < 0$, is described by the system of equations (10), if we put $\boldsymbol{j}(\boldsymbol{k}_\perp,z,\omega) = 0$, $\varepsilon_0(\omega) = 1$. In what follows we consider only that portion of the electromagnetic field in vacuum, which corresponds to a surface wave whose field is localised near the boundary of the conductor. Thus, we seek a solution of the modified system of equations (10) provided that

$$k_\perp c > |\omega|. \tag{22}$$

For such $k_\perp$ and $\omega$ we have the solution:

$$B_\varphi(\boldsymbol{k}_\perp,z,\omega) = B_\varphi(\boldsymbol{k}_\perp, z=-0,\omega)\exp(\kappa_0 z), \tag{23}$$

$$E_\rho(\boldsymbol{k}_\perp,z,\omega) = -i\frac{c\kappa_0}{\omega} B_\varphi(\boldsymbol{k}_\perp, z=-0,\omega)\exp(\kappa_0 z), \tag{24}$$

$$E_z(\boldsymbol{k}_\perp,z,\omega) = -\frac{ck_\perp}{\omega} B_\varphi(\boldsymbol{k}_\perp, z=-0,\omega)\exp(\kappa_0 z), \tag{25}$$

where $\kappa_0 = \sqrt{k_\perp^2 - \omega^2/c^2}$ and $B_\varphi(\boldsymbol{k}_\perp, z=-0,\omega)$ is the unknown function. To determine the functions $B_\varphi(\boldsymbol{k}_\perp, z=+0,\omega)$ and $B_\varphi(\boldsymbol{k}_\perp, z=-0,\omega)$ we use the conditions of continuity of the tangential components of the electromagnetic field at the boundary of the conductor. Equating the components $B_\varphi(\boldsymbol{k}_\perp,z,\omega)$ and $E_\rho(\boldsymbol{k}_\perp,z,\omega)$ in the plane $z = 0$, from formulas (18), (19), (23), (24), we find

$$B_\varphi(\boldsymbol{k}_\perp, z=-0,\omega) = B_\varphi(\boldsymbol{k}_\perp, z=+0,\omega)$$
$$= \frac{k_\perp\omega_p^2}{(\omega+i\nu_s)c[\kappa + \kappa_0\varepsilon(\omega)]}\frac{\Phi(\boldsymbol{k}_\perp, z=0,\omega)}{e}. \tag{26}$$

Relations (23)–(26) completely determine the Fourier transforms of the components of the low-frequency field localised at the conductor surface in vacuum. These Fourier transforms and the transforms described by formulas (18)–(20) are proportional to the Fourier transform of the ponderomotive potential on the conductor surface $\Phi(\boldsymbol{k}_\perp, z=0,\omega)$. For the ponderomotive potential (5) the Fourier transform has the form

$$\Phi(\boldsymbol{k}_\perp,z,\omega) = \frac{e^2}{m}\frac{\pi R^2}{|\omega_0 + ic\kappa_L(\omega_0)|^2}$$
$$\times\exp\left[-2\mathrm{Re}\,\kappa_L(\omega_0)z - \frac{k_\perp^2R^2}{4}\right]\int_{-\infty}^{+\infty} dt\boldsymbol{E}_L^2(t)\exp(i\omega t). \tag{27}$$

Expressions (18)–(27) allow us to find the electromagnetic field of the surface wave in vacuum and conductor. Equations (23)–(25) are suitable for describing only the part of the field localised at the surface of the conductor. This part of the field is determined by the Fourier transforms of the fields with sufficiently large wave vectors in a plane that is coplanar to the surface of the conductor: $k_\perp c > |\omega|$ (22). Therefore, the dependence of the field on coordinate $\boldsymbol{\rho}$ recovered by using the inverse Fourier transform in $\boldsymbol{\rho}$ (9) is bounded below by the region of integration in $k_\perp$ by the quantity $|\omega|/c$. Then, from (18), (22), (26) and (27) for the frequency-dependent azimuthal component of the Fourier transform of the magnetic field localised at the surface of the conductor, we obtain

$$B_\varphi(\boldsymbol{r},\omega)=\frac{\omega_p^2}{|\omega_0+ic\kappa_L(\omega_0)|^2}\frac{e}{mc}\frac{\pi R^2}{\omega+i\nu_s}\int_{\omega/c}^{\infty}\frac{k_\perp^2\,dk_\perp}{2\pi}\frac{J_0(k_\perp\rho)}{\kappa+\kappa_0\varepsilon(\omega)}$$

$$\times\exp\left(-\frac{k_\perp^2R^2}{4}\right)[\eta(-z)\exp(\kappa_0 z)+\eta(z)\exp(-\kappa z)]$$

$$\times\int_{-\infty}^{+\infty}dt\boldsymbol{E}_L^2(t)\exp(i\omega t),\ \omega>0, \tag{28}$$

where $\eta(z)$ is the unit Heaviside step function and $J_0(k_\perp\rho)$ is the zero order Bessel function. In the denominator of formula (28) we have the function $\kappa+\kappa_0\varepsilon(\omega)$, which, taking into account the explicit expressions for $\kappa_0$ and $\kappa$, can be written in the form

$$\kappa+\kappa_0\varepsilon(\omega)=\frac{1-\varepsilon^2(\omega)}{\kappa-\kappa_0\varepsilon(\omega)}\left[k_\perp^2-\frac{\omega^2}{c^2}\frac{\varepsilon(\omega)}{\varepsilon(\omega)+1}\right]. \tag{29}$$

Equation (29) is equal to zero if

$$k_\perp^2=\frac{\omega^2}{c^2}\left[1+\frac{1}{|\varepsilon'(\omega)|-1-i\varepsilon''(\omega)}\right], \tag{30}$$

where $\varepsilon''(\omega)=\omega_p^2\nu_s/\left[\omega(\omega^2+\nu_s^2)\right]+\varepsilon_0''(\omega)>0$, and we take into account that for the frequently realised conditions $\omega_p^2\gg(\omega^2+\nu_s^2)\,|\varepsilon_0'(\omega)|$ and $|\varepsilon'(\omega)|=-\varepsilon'(\omega)=\omega_p^2/(\omega^2+\nu_s^2)-\varepsilon_0'(\omega)>0$. Note that at low frequencies the absolute value of the real part of the dielectric constant is usually much greater than unity, $|\varepsilon'(\omega)|\gg1$, and in the denominator of (30) we can neglect the unity:

$$k_\perp\simeq\frac{\omega}{c}\left[1+\frac{1}{2}\frac{1}{|\varepsilon'(\omega)|-i\varepsilon''(\omega)}\right]. \tag{31}$$

Expressions (30) and (31) detemine the dispersion law for the waves propagating along the surface of the conductor (see, for example, [4]). Thus, the expression under the integral in (28) has a simple pole in the plane of the complex variable $k_\perp$. Consider the low-frequency field at large distances from the focal spot region when the inequalities $\rho\gg R$, $c/\omega$ are fulfilled. In this case, in calculating the integral over the variable $k_\perp$ we can use the asymptotic representation of the Bessel function:

$$J_0(k_\perp\rho)\approx\sqrt{\frac{2}{\pi k_\perp\rho}}\cos\left(k_\perp\rho-\frac{\pi}{4}\right),\ k_\perp\rho\gg1. \tag{32}$$

To calculate the integral in $k_\perp$, we choose in (28) the path of integration in the plane $k_\perp$, as shown in Fig. 1. The point in Fig. 1 denotes the pole corresponding to the surface wave (30), (31). The integral along the arc of an infinitely large radius is zero. The integral along the ray originating from point $\omega/c$ at an angle $\pi/4$ to the real axis is exponentially small at $\rho\gg R$. Therefore, the main contribution to the desired integral (28) comes from the residue at the pole. Taking into account the contribution from the pole (31) and formula (32), we find from (28) the expression for the Fourier transform of the azimuthal component of the magnetic field on the surface of the conductor:

$$B_\varphi(\rho,z=0,\omega)\simeq-\frac{e}{mc(\omega+i\nu_s)}\sqrt{\frac{\pi}{2}}\frac{\omega_p^2}{|\omega_0+ic\kappa_L(\omega_0)|^2}\left(\frac{\omega R}{c}\right)^2\times$$

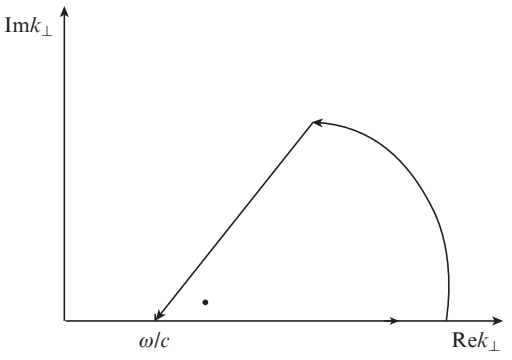


**Figure 1.** Contour of integration in formula (28).

$$\times[|\varepsilon'(\omega)|-i\varepsilon''(\omega)]^{-3/2}\sqrt{\frac{c}{\omega\rho}}\exp\left\{i\frac{\pi}{4}+i\frac{\omega}{2c}\rho\right.$$

$$\left.\times\left[2+\frac{1}{|\varepsilon'(\omega)|-i\varepsilon''(\omega)}\right]-\frac{\omega^2R^2}{4c^2}\left[1+\frac{1}{|\varepsilon'(\omega)|-i\varepsilon''(\omega)}\right]\right\}$$

$$\times\int_{-\infty}^{+\infty}dt\boldsymbol{E}_L^2(t)\exp(i\omega t),\ \omega>0. \tag{33}$$

Completely analogous to (23)–(25) we find the Fourier transforms of the components of the electromagnetic field in vacuum:

$$E_z(\boldsymbol{r},\omega)=-B_\varphi(\boldsymbol{r},\omega),$$

$$E_\rho(\boldsymbol{r},\omega)=-\frac{i}{\sqrt{|\varepsilon'(\omega)|-i\varepsilon''(\omega)}}B_\varphi(\boldsymbol{r},\omega), \tag{34}$$

$$B_\varphi(\boldsymbol{r},\omega)\simeq B_\varphi(\rho,z=0,\omega)\exp\left[\frac{\omega z}{c\sqrt{|\varepsilon'(\omega)|-i\varepsilon''(\omega)}}\right],\ z<0,\omega>0,$$

and from (18)–(20) with (26) and (27) taken into account, we find same values in the conductor:

$$E_z(\boldsymbol{r},\omega)=\frac{1}{|\varepsilon'(\omega)|-i\varepsilon''(\omega)}B_\varphi(\boldsymbol{r},\omega),$$

$$E_\rho(\boldsymbol{r},\omega)=-\frac{i}{\sqrt{|\varepsilon'(\omega)|-i\varepsilon''(\omega)}}B_\varphi(\boldsymbol{r},\omega), \tag{35}$$

$$B_\varphi(\boldsymbol{r},\omega)\simeq B_\varphi(\rho,z=0,\omega)\exp\left[-\frac{\omega z}{c}\sqrt{|\varepsilon'(\omega)|-i\varepsilon''(\omega)}\right],$$

$$z>0,\ \omega>0.$$

Expressions (33)–(35) describe the surface wave diverging from the focal spot. The amplitude of this wave decreases with distance proportionally to $1/\sqrt{\rho}$. According to (33), the presence of dissipation, caused by collisions of electrons and by the field absorption by the lattice and bound electrons, leads to a decay of the surface wave at large distances, when

$$\rho\geqslant\rho_m\simeq2\frac{c}{\omega}\frac{|\varepsilon'(\omega)|^2+\varepsilon''^2(\omega)}{\varepsilon''(\omega)}. \tag{36}$$

Therefore, we will consider the characteristics of the surface wave in the region $\rho<\rho_m$, when a change in the wave amplitude due to dissipation can be neglected. This region exists if

$\rho_m \gg R, c/\omega$. Note that the region of localisation of the surface wave field in vacuum

$$\delta_v \simeq \frac{c}{\omega\sqrt{2}}\{[\varepsilon'^2(\omega)+\varepsilon''^2(\omega)]^{1/2}+|\varepsilon'(\omega)|\}^{1/2} \quad (37)$$

is much greater than the penetration depth into the conductor:

$$\delta_m \simeq \delta_v[\varepsilon'^2(\omega)+\varepsilon''^2(\omega)]^{-1/2} \ll \delta_v. \quad (38)$$

## 5. Physical characteristics of the surface wave

To calculate the energy $W$, transported by the surface wave, we consider a cylindrical surface of radius $\rho$ and length $dz$. The symmetry axis of this surface coincides with the propagation direction of the laser pulse and passes through the origin of the coordinates. During all the time, through this surface along the normal, the energy passes that is equal to the product of the time-integrated energy flux density

$$\boldsymbol{P}(\boldsymbol{r}) = \int_{-\infty}^{+\infty} dt \frac{c}{4\pi}[\boldsymbol{E}(\boldsymbol{r},t)\boldsymbol{B}(\boldsymbol{r},t)] \quad (39)$$

and the element of sites $2\pi\rho dz$:

$$dW = 2\pi\rho dz \int_0^\infty d\omega \frac{c}{8\pi^2}\{[\boldsymbol{E}(\boldsymbol{r},\omega)\boldsymbol{B}^*(\boldsymbol{r},\omega)]+\text{c. c.}\}. \quad (40)$$

By integrating expression (40) in the $z$ coordinate from $-\infty$ to $+\infty$ and using relations (34) and (35), we find the energy of surface waves per unit frequency interval $d\omega$:

$$\frac{dW}{d\omega} = \frac{c\rho}{2\pi}\Big[\int_{-\infty}^{0} dz|B_\varphi(\boldsymbol{r},\omega)|^2$$

$$-\frac{|\varepsilon'(\omega)|}{\varepsilon'^2(\omega)+\varepsilon''^2(\omega)}\int_0^{+\infty} dz\,|B_\varphi(\boldsymbol{r},\omega)|^2\Big]. \quad (41)$$

From formula (41) and relations (34) and (35) it follows that the energy of the surface wave in vacuum is much higher than the energy in the conductor. By calculating in formula (41) the integral over the area of vacuum, we obtain the spectral energy distribution of surface waves

$$\frac{dW}{d\omega} = \frac{\omega_p^4}{|\omega_0+ic\kappa_L(\omega_0)|^4}\frac{\sqrt{2}e^2R^4}{8m^2c^3}$$

$$\times\frac{\omega^2}{\omega^2+\nu_s^2}\Big[\int_{-\infty}^{+\infty} dt\boldsymbol{E}_L^2(t)\exp(i\omega t)\Big]^2$$

$$\times\frac{1}{\varepsilon'^2(\omega)+\varepsilon''^2(\omega)}\Big[\sqrt{\varepsilon'^2(\omega)+\varepsilon''^2(\omega)}+|\varepsilon'(\omega)|\Big]^{-1/2}$$

$$\times\exp\Big\{-\frac{\omega^2R^2}{2c^2}\Big[1+\frac{|\varepsilon'(\omega)|}{\varepsilon'^2(\omega)+\varepsilon''^2(\omega)}\Big]\Big\},\ \omega>0. \quad (42)$$

According to (42), the spectral energy distribution depends not only on the physical characteristics of the conductor, but also on the shape of the incident laser pulse. Let us investigate in more detail the spectral composition of the generated field for the frequently discussed case when the pulse shape is described by a Gaussian distribution:

$$\boldsymbol{E}_L^2(t) = E_L^2\exp(-t^2/\tau^2). \quad (43)$$

Consider distribution (42) under conditions typical of many experiments, when the inequalities

$$\frac{\omega_p^2}{\omega^2+\nu_s^2} \gg |\varepsilon_0'(\omega)|\,,\ \frac{\omega_p^2}{\omega^2+\nu_s^2}\frac{\nu_s}{\omega} \gg |\varepsilon_0''(\omega)|,$$

$$\omega_0 \gg \nu_h,\ \frac{\omega_p^2}{\omega_0^2} \gg |\varepsilon_0'(\omega_0)| \quad (44)$$

are met.

For a pulse (43) under conditions (44), expression (42) takes the form

$$\frac{dW}{d\Omega} = \frac{8\sqrt{2}e^2}{\sqrt{L^2+R^2}}\frac{W_L^2}{m^2c^4}\frac{1}{\omega_p^5\tau_*^5}I(\Omega), \quad (45)$$

where $\Omega = \omega\tau_*$ is the dimensionless frequency; $W_L = \sqrt{\pi}E_L^2R^2L/8$ is the laser pulse energy; and the dimensionless function

$$I(\Omega) = \frac{\Omega^{9/2}\sqrt{\Omega^2+\gamma_s^2}}{\sqrt{\Omega+\sqrt{\Omega^2+\gamma_s^2}}}\exp\Big(-\frac{\Omega^2}{2}\Big),\ \gamma_s = \nu_s\tau_*. \quad (46)$$

Here, the parameter $\gamma_s$ accounts for the effect of electron collisions on the distribution of energy over the frequencies. Function (46) describing the spectral energy distribution of the surface wave is shown in Fig. 2 for different values of the dimensionless collision frequency $\gamma_s$. It is seen that the emission spectrum has a broad maximum, the position of which depends weakly on the parameter $\gamma_s$. However, with an increase in the collision frequency, the maximum amplitude is increased. To explain this behaviour, consider function (46) in more detail. When $\gamma_s \ll 1$, which corresponds to the limit of rare collisions, from formula (46) we obtain the expression

$$I(\Omega) \simeq \frac{\Omega^5}{\sqrt{2}}\exp\Big(-\frac{\Omega^2}{2}\Big). \quad (47)$$

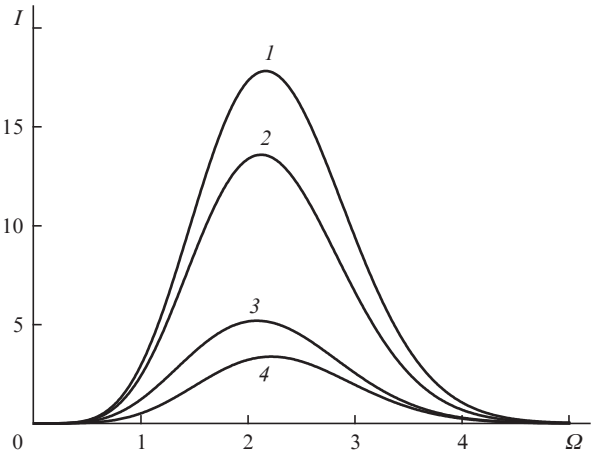


**Figure 2.** Dependences of the normalised spectral energy density $I(\Omega)$ (46) for surface waves on the dimensionless frequency $\Omega$ at $\gamma_s = (1)$ 8, (2) 4, (3) 1 and (4) 0.25.

In this case, the spectral distribution has a maximum at $\Omega_{\max} \simeq \sqrt{5}$, which corresponds to the frequency

$$\omega_{\max} = \frac{\sqrt{5}}{\tau\sqrt{1+R^2L^2}}. \tag{48}$$

If during the laser pulse action there are many collisions between the electrons ($\gamma_s \gg 1$), from formula (46) we have the relation

$$I_s(\Omega) \simeq \sqrt{\gamma_s}\,\Omega^{9/2}\exp\left(-\frac{\Omega^2}{2}\right). \tag{49}$$

Function (49) has a maximum at $\Omega_{\max} = 3/\sqrt{2}$, which corresponds to the frequency

$$\omega_{\max} = \frac{3}{\sqrt{2}\tau\sqrt{1+R^2/L^2}}. \tag{50}$$

Frequencies (48) and (50) differ slightly, which corresponds to the data shown in Fig. 2. In the case of tightly focused laser radiation $R \ll L$, and the position of the maximum of the spectral distribution is determined by the inverse duration of the laser pulse: $\omega_{\max} \sim 1/\tau$. With an increase in the size of the focal spot, the maximum is shifted to lower frequencies $\omega_{\max} \sim c/R$. Also, in accordance with Fig. 2, from formula (49) we see that in the limit of frequent electron collisions the maximum of the function $I(\Omega)$ increases proportionally to $\sqrt{\gamma_s}$.

By integrating expression (45) over the frequencies, we find the total energy of the surface waves

$$W = \frac{8\sqrt{2}\,e^2}{L}\frac{W_L^2}{m^2c^4}\frac{w}{\omega_p^5\tau^5(1+R^2L^2)^3}, \tag{51}$$

where

$$w = \int_0^\infty d\Omega\Omega I(\Omega) = \int_0^\infty d\Omega\frac{\Omega^{9/2}\sqrt{\Omega^2+\gamma_s^2}}{\sqrt{\Omega+\sqrt{\Omega^2+\gamma_s^2}}}\exp\left(-\frac{\Omega^2}{2}\right). \tag{52}$$

From formula (51) we see that at a fixed energy and duration of the laser pulse, the energy of the surface wave is maximum upon tight focusing when the condition $R \ll L$ is fulfilled. The dependence of the normalised energy of surface waves (52) on the the electron collision frequency is presented in Fig. 3. For large values of $\gamma_s$ the energy increases proportionally to $\sqrt{\gamma_s}$. Using approximate formulas (47) and (49), we obtain explicit expressions for $w$ at small and large values of $\gamma_s$. In the limit of rare collisions of the electrons, when $\gamma_s \ll 1$, by integrating (47) in $\Omega$, we find the relation

$$w = \int_0^\infty d\Omega\frac{\Omega^5}{\sqrt{2}}\exp\left(-\frac{\Omega^2}{2}\right) = \frac{8}{\sqrt{2}} \simeq 5.7. \tag{53}$$

In the limit of frequent collisions, when $\gamma_s \gg 1$, and for the normalised energy of surface waves, from (52) we have the expression

$$w = \sqrt{\gamma_s}\int_0^\infty d\Omega\Omega^{9/2}\exp\left(-\frac{\Omega^2}{2}\right)$$

$$= 2^{7/4}\frac{21}{16}\Gamma\left(\frac{3}{4}\right)\sqrt{\gamma_s} \simeq 5.4\sqrt{\gamma_s}. \tag{54}$$

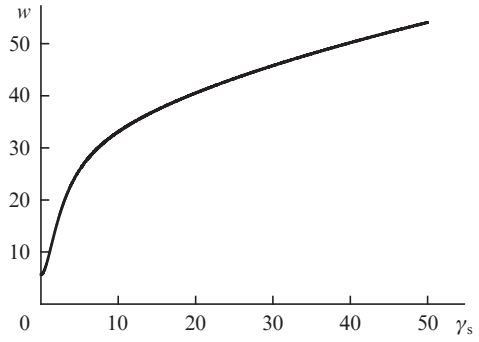


**Figure 3.** Dependence of the normalised energy of surface waves $w$ (52) on the parameter $\gamma_s$.

Let us analyse the spatiotemporal structure of the surface wave on the conductor surface, where $z = 0$. By using an inverse Fourier transform with respect to time, from formulas (33) and (43) we find the distribution of the magnetic field of the surface wave

$$B_\varphi(\rho, z=0, t) = -\frac{eE_L^2R^2\tau}{2\sqrt{2}\,mc(c\tau_*)^{3/2}(\omega_p\tau_*)^3}\frac{H(\xi)}{\sqrt{\rho}}, \tag{55}$$

$$H(\xi) = 2\mathrm{Re}\int_0^\infty dz z^3\sqrt{z+i\gamma_s}\exp\left(i\frac{\pi}{4}+iz\xi-\frac{z^2}{4}\right), \tag{56}$$

where $\xi = (\rho/c - t)/\tau_*$ and use is made of the identity $B_\varphi(\rho, z = 0, -\omega) = B_\varphi^*(\rho, z = 0, \omega)$. Dependence (56) is shown in Fig. 4 for two values of the dimensionless frequency of electron collisions, $\gamma_s$. Curve (*2*) corresponds to the limit when the collision frequency is less than $1/\tau_*$. An increase in the frequency of collisions leads to an increase in the amplitude of the generated magnetic field, the spatiotemporal profile of the surface wave being also modified [curve (*1*) in Fig. 4]. In the limit of frequent collisions, when $\gamma_s \gg 1$, from (56) we find the expression

$$H(\xi) = -2\sqrt{\pi\gamma_s}\frac{d^3}{d\xi^3}\exp(-\xi^2)$$

$$= -8\sqrt{\pi\gamma_s}\xi(3-2\xi^2)\exp(-\xi^2). \tag{57}$$

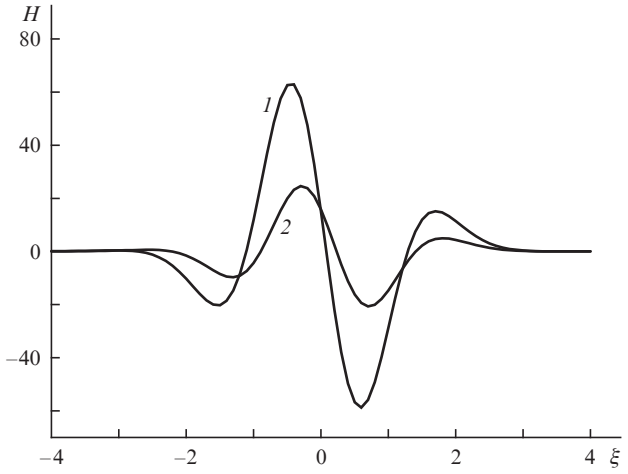


**Figure 4.** Spatiotemporal structure of the magnetic field of the surface wave (56) at $\gamma_s$ = (*1*) 8 and (*2*) 0.25.

It follows from Fig. 4 and formulas (56) and (57) that the surface wave propagates along the surface of the conductor in the form of an electromagnetic pulse with a duration of the order of $\tau_*$. Upon tight focusing of laser radiation $R \ll L$, and the pulse duration of the surface wave is comparable to the duration of the laser pulse. The surface wave pulse duration increases with increasing size of the focal spot, and when $R \gg L$, becomes equal to $R/c$.

## 6. Conclusions

Consider the energy of the surface waves for typical parameters of laser irradiation of the conductor. To do this, we rewrite formula (51) with regard to the expression $W_L = I_L \pi^{3/2} R^2 \tau$:

$$W = 8\sqrt{2}\,\pi^3 \frac{e^2\omega_p}{c}\left(\frac{I_L}{m\omega_p^3}\right)^2 \frac{R^4 L^2}{(R^2+L^2)^3} w, \qquad (58)$$

where $I_L = cE_L^2/(8\pi)$ is the flux density of laser radiation. Energy (58) under the condition $R^2 = 2L^2$ has a maximum value

$$W_{max} \approx 52 \frac{e^2\omega_p}{c}\left(\frac{I_L}{m\omega_p^3}\right)^2 w. \qquad (59)$$

Let us estimate the energy and frequency of the generated surface waves. As a target we use a semiconductor with the plasma frequency $\omega_p \approx 2\times10^{14}$ s$^{-1}$ and the electron collision frequency $\nu_s \approx 10^{13}$ s$^{-1}$. We assume that the flux density is $I_L \approx 10^{12}$ W cm$^{-2}$, the pulse duration is $\tau \approx 400$ fs, and the carrier frequency is $\omega_0 \approx 2\times10^{14}$ s$^{-1}$. Strictly speaking, when $\omega_0 \approx \omega_p$, formula (59) requires clarification. However, from the comparison of expression (59) with the results obtained in [13] at $\omega_0 > \omega_p$, we can conclude that the optimal conditions for generation are achieved at $\omega_0 \approx \omega_p$, and formula (59) is suitable for the estimates even at such frequencies. For the parameters used, the pulse length is $L \approx 120$ μm and $R \approx 170$ μm. The parameter characterising the influence of the collisions is $\gamma_s = 7$, and in accordance with Fig. 3, $w = 30$. Under these conditions, according to formula (50), the maximum emission occurs at a frequency of 0.5 THz, and the total radiation energy (59) is $0.5\times10^{-12}$ J. Since the total energy in the pulse is equal to $6\times10^{-4}$ J, the conversion efficiency is very small, i.e., about $10^{-9}$. At the same time, as is seen from relation (59), in conductors with a lower plasma frequency and at a higher intensity of radiation, the generation efficiency can be significantly enhanced. However, one should not choose too high intensity due to the efficient heating of electrons and, subsequently, of the lattice. Note also that in metals, where the plasma frequency is high, the generation efficiency of surface waves at the ponderomotive impact of the focused laser pulse radiation incident along the normal to the sample surface is less than in semiconductors.

***Acknowledgements.*** This work was supported by the Russian Foundation for Basic Research (Grant No. 12-02-00744) and by the RAS Presidium (Programme No. 24).

## References

1. Raether H.R. *Surface Plasmons on Smooth and Rough Surfaces and on Gratings* (New York: Springer-Verlag, 1988) Vol. 111.
2. Irvine S.E., Elezzabi A.Y. *Appl. Phys. Lett.*, **86**, 264102 (2005).
3. Welsh G.H., Wynne K. *Opt. Express*, **17**, 2470 (2009).
4. Mayer S.A. *Plasmonics: Fundamentals and Applications* (New York: Springer, 2007).
5. Kim S., Jin J., Kim Y.-I., Park Y.-J., Kim Y., Kim S.W. *Nature*, **453**, 757 (2008).
6. Kadlec F., Kuzel P., Coutaz J.-L. *Opt. Lett.*, **29**, 2674 (2004).
7. Kroo N., Farkas Gy., Dombi P., Varro S. *Opt. Express*, **16**, 21656 (2008).
8. Ionin A.A., Kudryashov S.I., Seleznev L.V., Sinitsyn D.V., Emelyanov V.I. *Pis'ma Zh. Eksp. Teor. Fiz.*, **97**, 139 (2013).
9. Parashar J., Pandey H.D., Tripathi V.K. *J. Plasma Phys.*, **59**, 97 (1998).
10. Wang X.Y., Downer M.C. *Opt. Lett.*, **17**, 1450 (1992).
11. Kudryashov S.I., Emelyanov V.I. *Pis'ma Zh. Eksp. Teor. Fiz.*, **73**, 751 (2001) [*JETP Lett.*, **73**, 666 (2001)].
12. Lindgren T., Larsson J., Stenflo L. *Plasma Phys.*, **24**, 1177 (1982).
13. Frolov A.A. *Fiz. Plazmy*, **33**, 206 (2007).
14. Gurzhi R.N. *Zh. Eksp. Teor. Fiz.*, **35**, 965 (1958) [*Sov. Phys. JETP*, **8**, 673 (1959)].